Enhancing Torsional Behavior of Deep Beams Strengthened with NSM Steel and Basalt Bars under Repeated Pure Torsion

Noor M. Salih
Civil Engineering Department, Mustansiriyah University, Baghdad, Iraq
noormohamed@uomustansiriyah.edu.iq (corresponding author)

Waleed A. Waryosh
Civil Engineering Department, Mustansiriyah University, Baghdad, Iraq
waleedwaryosh@uomustansiriyah.edu.iq

Received: 16 May 2025 | Revised: 6 June 2025 and 15 June 2025 | Accepted: 17 June 2025

 DOI: https://doi.org/10.48084/etasr.12199

ABSTRACT

This study investigates the torsional behavior of reinforced concrete deep beams enhanced through the Near-Surface Method (NSM), using steel and basalt bars under repeated torsional loads. Five beam specimens were cast and tested. One served as the unstrengthened reference, while the remaining four were reinforced using NSM bars on either two or four sides. The experimental program investigated the impact of reinforcing material (steel and basalt) and several strengthened faces. The results demonstrated that the NSM strengthening significantly enhanced the beams' torsional resistance. When evaluated with the reference beam, the ultimate torque increased by 16.5% and 30.4% for the two-sided and four-sided steel structures, respectively, while the basalt bars exhibited enhancements of 33.0% and 46.0%, respectively. Furthermore, the longitudinal elongation at failure decreased by as much as 22.3% in the most effective configurations, indicating a significant enhancement in the deformation control. The study indicates that augmenting the number of reinforced faces and employing basalt bars achieves beneficial results in terms of strength and stiffness.

Keywords-deep beam; pure torsion; NSM strengthening; basalt bar; repeated loads

I. INTRODUCTION

Deep beam is a structural element with a significant depth compared to its span length and a relatively slender width. Reinforced concrete deep beams are prevalent and significant components of large structures and superstructures, such as bridges, offshore constructions, and large multistory buildings. Their main purpose is to transmit loads to foundations, transfer girders, pile caps, bent caps, and some walls. The ACI 318-19 [1] defines a deep beam as a structural element that is loaded on one face and supported on the other face. A strut compression element can be established between the load and the support, provided that one of the following conditions is satisfied: (1) the clear span does not exceed four times the total member depth (h), or (2) concentrated loads are present within a distance of $2h$ from the support face. Repeated loading (cyclic loading), commonly encountered in real-life structures, can influence the collapse load factor. There are two main classes of cyclic loadings, with the first known as low-cycle loading, involving significant bond stress fluctuations in less than 100 cycles. Low cycle loadings are the consequence of strong seismic activity and wind forces. High-cycle or fatigue loading is the second type characterized by a large number of cycles, often in the hundreds of thousands or millions, applied at relatively low bond stress levels. The structural elements supporting the vibrating machinery and bridge elements in offshore structures often experience severe fatigue loads. [2].

Concrete is weak in torsion, still some concrete structures are subjected to torque. To enhance the torsional resilience of reinforced concrete beams, it is essential to confront the structural failure or damage caused by increasing applied loads. The NSM is a novel strengthening technique that involves placing reinforcement into grooves formed in the concrete cover zone. It enhances the torsional strength with the use of epoxy and cement-based glue [3, 4]. The preliminary experiment utilizing this technique was conducted in the early 1950s. Nonetheless, this technique is currently regarded as a contemporary concept. NSM offers advantages, such as reduced susceptibility to environmental factors like fire, along with a shorter application time compared to other techniques. Moreover, it is less susceptible to debonding failure in the concrete [5, 6]. Several studies have investigated the NSM technique for strengthening the reinforced concrete members using Fiber Reinforced Polymer (FRP) bars [7, 8]. The greater tensile strength of FRP and its corrosion resistance relative to

steel are its main advantageous properties, making it suitable for strengthening works. Nonetheless, these reasons are not sufficient to exclude steel from the NSM method, particularly given its higher modulus of elasticity. Basalt Fiber Reinforced Polymer (BFRP) bars are a relatively new development compared to other FRP bars, offering several advantages, such as better performance in extreme temperatures, chemical resistance, lower cost, and enhanced environmental sustainability [9, 10].

Authors in [11] examined the torsional performance of thin-walled tubular strengthened concrete beams enhanced by NSM with Carbon Fiber Reinforced Polymer (CFRP) bars. The results indicated that the CFRP bars significantly improved the twisted beam's torsional strength, stiffness, and ductility. The CFRP bar reached 89% of its maximum tensile strength, demonstrating its effectiveness in resisting torsion. It was also found that strengthening led to an increased crack propagation but reduced crack width. The performance of reinforced concrete beams under combined torsional and bending loads, reinforced with NSM steel bars in various combinations was investigated in [12]. The experimental program consisted of seven beams, with one unreinforced reference beam. A significant increase in the torque of the conventional beam was detected, with the test beam incorporating a 10 mm anchored NSM steel bar at a 90-degree angle and 100 mm spacing achieving the highest increase of 44.19%. Authors in [13] investigated the effectiveness of strengthening reinforced concrete beams under torsional loads. They evaluated thirteen specimens, including control and improved beams, under various parameters. The results indicated that most reinforced beams had 9% fewer cracks than the reference beam. The CFRP bars performed better than the NSM steel rebar, especially when spaced 130 mm apart.

Substituting carbon bars with steel bars decreased the rotation by 4% and raised the ultimate torsional strength by 3.5%. The strengthening also enhanced the energy absorption and ductility. Authors in [14] conducted a numerical analysis on specimens, including one control beam and two strengthened beams with different configurations. The results showed a convergence in the failure patterns and final torque. The maximal torque increased by 18.06% when the beams were reinforced with U-shaped stirrups and NSM closed stirrups at a spacing of 130 mm. Nonetheless, few studies have specifically addressed the torsional strengthening, and the application of NSM for pure torsion in deep beams remains largely unexplored.

This study investigates how deep beams behave under pure torsion when strengthened with NSM steel or basalt bars applied in different configurations. The objectives include evaluating the torsional performance, cracking behavior, and ductility of NSM-strengthened reinforced concrete deep beams.

II. EXPERIMENTAL PROGRAM

A. Properties of Materials

1) Concrete

Concrete made from Ordinary Portland Cement (OPC) was utilized for casting the beams, and its properties were carefully studied using standardized testing procedures in accordance with Iraqi Standard (IQS) and ASTM standards. This study investigated a Type I OPC, which was maintained in a dry state to protect it against various weather conditions. The test results revealed that the cement complied with IQS (No. 5/1984) [15] and ASTM C150-17 [16]. Natural sand with the maximum particle size of 4.75 mm was utilized as the fine aggregate, following the required evaluation. The graded fine aggregate satisfied the zone standards of IQS No. 45/1984 and ASTM C128-15. In compliance with the Iraqi laws, local gravel was crushed, and several concrete mixtures with a maximum particle size of 12.5 mm were formulated. Every piece of crushed gravel was carefully cleaned, maintained in a dry state for a prolonged duration, and thereafter encased in plastic in accordance with IQS No. 45/1984 [17]. Tap water was utilized for the mixing and curing of all concrete specimens.

2) Mixing NSC

Table I provides the composition ratios of the NSC used during this investigation.

TABLE I. CHARACTERISTICS OF NSC MIX

Water/Cement ratio	Cement (kg/m^3)	Water (L/m^3)	Fine aggregate (kg/m^3)	Aggregate (kg/m^3)
0.5	300	150	600	1050

Before mixing the NSC, it was essential to verify that the mixture was clean and somewhat moist, but not wet. The procedure started with the addition of gravel and sand into the mixture. One-third of the total water was used to hydrate the aggregates for 60 s. Thereafter, the cement was added and mixed for 30 s. Subsequently, an additional third of the water was added and mixed for 1 min. The residual water was gradually added and mixed for an additional min, ending in a total mixing time of 1.5 min. The entire process required four min to be completed. A 3000 kN.m universal compression machine tested the specimens for different mix types, determining the compression, modulus of rupture, splitting tensile strength, and modulus of elasticity based on the average of three samples. The tests were conducted in accordance with BS 1881-116:1983 [18] and the ASTM standards C293/C293M-16 [19], C496/C496M-17 [20], and C469-02 [21].

3) Reinforcement Bars

Two types of reinforcement bars were used in this study: Mild steel bar of 10 mm and 12 mm diameter, and Basalt bar of 10 mm diameter. The mechanical properties of the tested bars, are presented in Tables III and IV.

4) Test Specimens

The study consists of five 1200 mm long RC deep beams with a 200 mm × 400 mm rectangular cross-section, with clear span of 1000 mm. Each deep beam was reinforced with two Ø12 bars in tension, two Ø12 bars in compression, and two Ø12 bars placed at mid-depth. The beams were vertically reinforced with double-legged steel stirrups of a 10 mm diameter at 150 mm intervals.

TABLE II. SPECIFICATIONS OF THE CONTROL SAMPLES

Type of test	Quantity of specimens	Type of specimens	Dimensions (mm)	Average estimated value
Compression	3	Cubes	100×100×100	30.0 MPa
Modulus of elasticity	3	Cylinders	150×300	24.5 GPa
Splitting tensile strength	3	Cylinders	100×200	2.90 MPa
Modulus of rupture	3	Prisms	100×100×50	3.80 MPa

TABLE III. STEEL BARS PROPERTIES

Nominal diameter (mm)	Actual diameter (mm)	Yield stress f_y (MPa)	Ultimate strength	Elongation%	Modulus of elasticity (GPa)	Min limit of elongation (%)
10	9.80	495	708	15	200	9
12	11.9	560	715	14	200	9

TABLE IV. BASALT BAR PROPERTIES

Nominal diameter (mm)		Maximum tensile strength	Modulus of elasticity	Elongation at break min. value	Weight per meter
Outside diameter	Inside diameter	MPa	GPa	%	(gr/m)
10	8.8	950	55.00	2.5-3.2	125

TABLE V. TEST SPECIMEN DETAILS

Named of Specimens	Details
CRS0	Conventional concrete, reinforced by steel bars without strengthening
CRSNS2	Conventional concrete, reinforced by steel bars, strengthened with (NSM) by steel bars on 2 sides.
CRSNS4	Conventional concrete, reinforced by steel bars, strengthened with (NSM) by steel bars on 4 sides.
CRSNB2	Conventional concrete, reinforced by steel bars, strengthened with (NSM) by Basalt bars on 2 sides.

The clear cover for both the top and bottom reinforcement is 30 mm. Figures 1 and 2 illustrate the dimensions and reinforcement details of the control RC deep beam. Several variables were considered during testing, including the strengthening configuration and bar type. The samples were named as listed in Table V. The term two-side NSM strengthening refers to placing two bars on each of the two vertical faces of the beam, resulting in a total of four bars. In contrast, four-side NSM strengthening involves applying one bar on each of the four faces (top, bottom, and both vertical sides), also totaling four bars. The NSM bars used in both configurations were either steel or basalt, depending on the specimen.

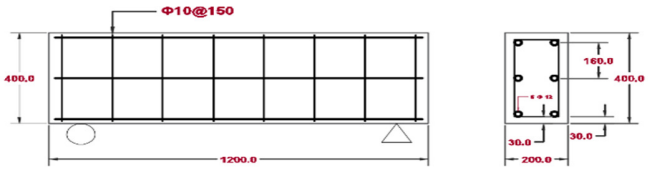

Fig. 1. Reinforcing details and dimensions of the specimens.

5) Strengthening Procedure

The current study utilized groove dimensions of 15×15 mm (width and depth) for embedding NSM bars. After 28 days of concrete curing, the wooden strips were removed from the grooves in the cover. The grooves were then cleaned to remove any debris. Epoxy adhesive was applied, filling the grooves to half of their depth, and the bars were placed and lightly pressed into position to ensure that the epoxy filled the space between the bars and the groove sides. Special attention was given to centering the bars within the grooves, followed by the uniform application of the adhesive layer between the steel bars and the beam surfaces. After placing the bars, the installation was completed by filling the grooves entirely with epoxy adhesive, followed by the application of an epoxy coating to ensure surface uniformity. The surface was then leveled using a steel blade.

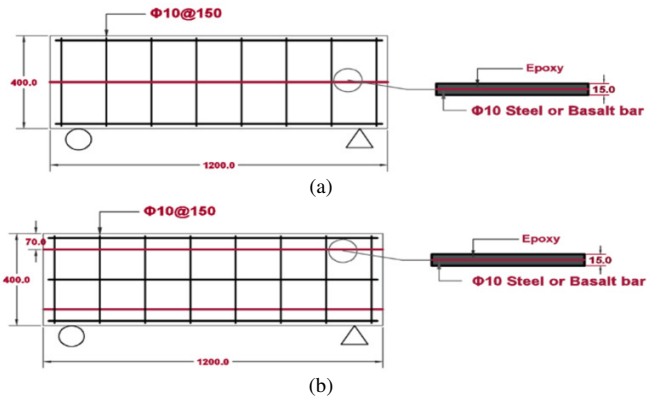

Fig. 2. Strengthening configurations of test specimens: (a) four-side NSM (b) two-side NSM.

6) Test Set-Up

The test setup was designed to apply pure torsional loading using a hydraulic testing system (EPP 300). The system generates a vertical force up to 3000 kN.m, which is transferred into torsional moments through a test setup involving two steel arms and a steel support frame, as shown in Figure 3. The girder transferred the vertical force, converting it into opposing torsional forces at both beam ends. The beam specimens were carefully positioned, and dial gauges were fixed to measure the twisting angle and longitudinal elongation. A rubber layer was

placed between the girder and the arms to ensure an even load distribution and minimize the stress concentration. The key components of the test setup are: (1) hydraulic jack, (2) steel box girder, (3) steel arms, (4 and 5) dial gauges, (6) supports, and (7) deep beam specimen. The reference beam specimen (CRS0.re) was tested under monotonic loads in incremental steps until failure occurred. Other beam specimens were tested under repeated loading with five cycles. The cycles of the repeated loading reached the required amplitude and then returned to the zero level. The torque range for all specimens was determined using a reference beam, with 60% as the upper limit of cyclic loading applied to both strengthened and unstrengthened specimens. If the beam specimen does not fail within the specified five cycles, the load continues to increase until failure.

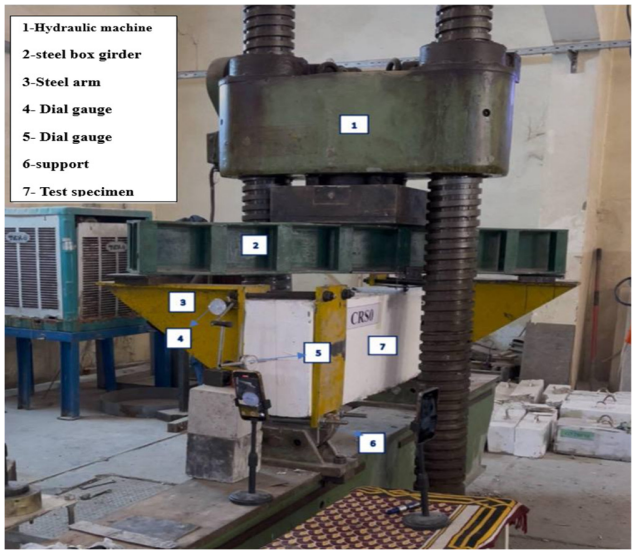

Fig. 3. Experimental setup for torsional testing.

III. RESULTS

A. Cracking Pattern and Mode of Failure

All of the specimens that were analyzed had their crack patterns photographed, as displayed in Figure 4. The results indicate that the beams strengthened with NSM bars showed an improved cracking behavior compared to the unstrengthened reference beams. CRSNS4 exhibited the finest and most uniformly distributed cracks due to increased face strengthening of the NSM method. CRSNB2 and CRSNB4 demonstrated delayed cracking and enhanced crack control, with CRSNB4 exhibiting finer cracks than CRSNB2. However, the cracks in the basalt-strengthened specimens were wider than in their steel equivalents, indicating a lower modulus of elasticity. The increased face strengthening of the NSM bars improved the crack distribution and decreased the width, especially with steel bars.

B. Ultimate Torsion Capacity

Figure 5 compares three specimens (CRS0, CRSNS2, and CRSNS4), showing improvements in torsional performance. CRS0 had a first torsional crack at 17.20 kN.m and an ultimate torsional strength of 24.73 kN.m. CRSNS2 showed a 39.9% increase in the torsional cracking moment (*Tcr*) and 16.5% increase in the applied factored torsional moment (*Tu*). These improvements are attributed to the strategic placement of NSM steel bars. CRSNB2 demonstrated a 31.3% improvement in both the first torsional crack (Tcr) and ultimate torsional strength (Tu), while CRSNB4 exhibited a 50.0% increase in Tcr and a 46.1% increase in Tu relative to the control specimen (CRS0). The results reveal significant improvements in each specimen.

Fig. 4. Failure modes and cracking patterns of the observed deep beam.

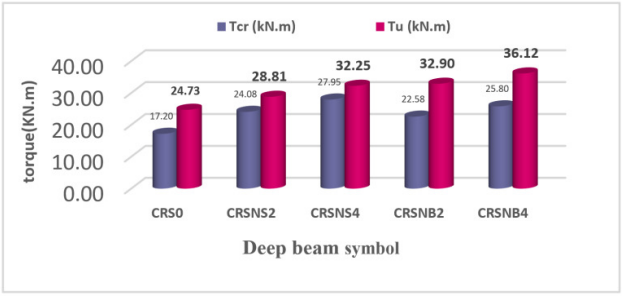

Fig. 5. Cracking and ultimate torque moment.

The results demonstrate the efficacy of basalt bars for enhancing both the cracking torque and ultimate torsional

resistance, especially when applied around the entire beam perimeter. In both, two-sided and four-sided NSM configurations, the specimens strengthened with basalt bars displayed a better torsional performance compared to those strengthened with steel bars. In the CRSNB2, a *Tu* of 32.90 kN.m was achieved, outperforming CRSNS2 (*Tu* = 28.81 kN.m) by approximately 14.2%. In the CRSNB4, a *Tu* of 36. 12 kN.m was achieved, while CRSNS4 recorded 32. 25 kN.m, reflecting an enhancement of 12.0%. *Tcr* decreased by around 10.4% in CRSNB2 compared to CRSNS2 and by about 7.7% in CRSNB4 compared to CRSNS4. Despite these improvements, early cracks can be seen in beams reinforced with basalt bars. These early cracks are attributed to the brittle nature and lack of yielding in basalt bars.

C. Angles of Twisting and Elongation

In comparison to the reference specimen CRS0, all four specimens exhibited significant reductions in torsional crack widths: 34.3% in CRSNS2, 45.7% in CRSNS4, 40.0% in CRSNB2, and 45.7% in CRSNB4, as presented in Figure 6.

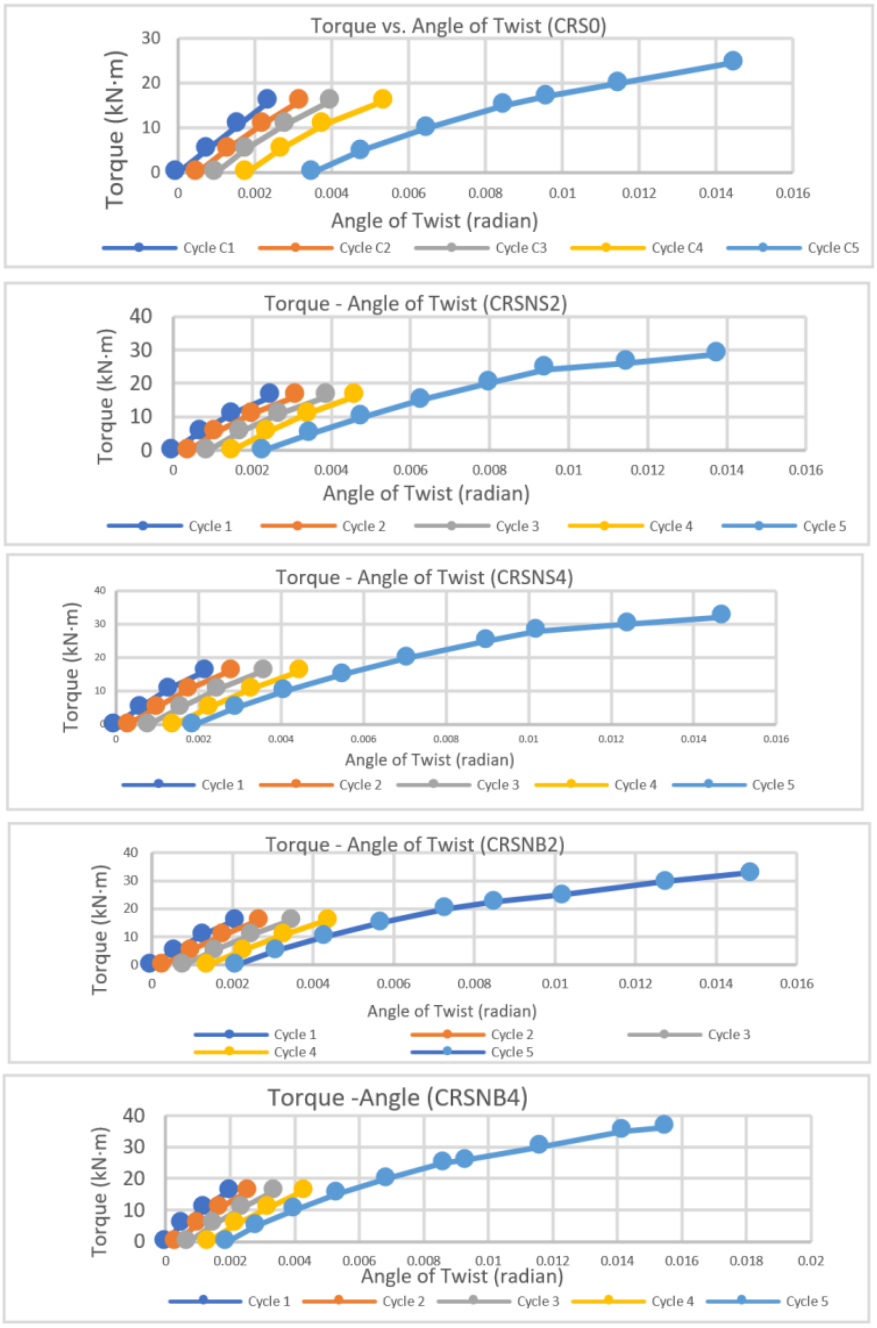

Fig. 6. Torque angle of twist.

Increasing the placement of NSM from two (CRSNS2) to four (CRSNS4) decreased the residual angle by 17.4%, highlighting the efficacy of the four-sided confinement. The basalt specimens showed a similar pattern, with CRSNB4 reducing the residual by 9.5% compared to CRSNB2. In a comparison of steel and basalt under similar configurations, CRSNB2 outperformed CRSNS2 by 8.7% in reducing the residual twist; however, CRSNB4 and CRSNS4 exhibited almost equivalent values, indicating that the strengthening distribution over all four faces is more important than the material type.

In Cycle 5, all specimens exhibited a transition from linear to nonlinear behavior following the first cracking, with the steel- reinforced models exhibiting a more gradual post-crack stiffness degradation, whereas the basalt samples experienced greater reductions due to their lower modulus of elasticity. In the elongation comparison between NSM steel and basalt, the CRSNS2 and CRSNS4 specimens showed reductions in elongation by 30% and 45%, respectively, and decreases in residuals by 35% and 50%, compared to CRS0, due to the effective crack restraint provided by the NSM steel bars. Additionally, CRSNB2 and CRSNB4 achieved reductions of 25% and 38% in elongation, as well as decreases of 30%–40% in residual twisting, while proving less effective than the steel ones due to lower basalt stiffness. All models demonstrated a linear response before the first cracking and a nonlinear response after cracking. CRSNS4 exhibited the smoothest nonlinear transition.

D. Stiffness

Torsional stiffness (*Kt*) refers to a structural member's resistance to twisting when subjected to an applied torque. It represents a characteristic of rigidity and is mathematically expressed as:

$$Kt = T / \theta \quad (1)$$

where T is the applied torque (kN.m) and θ is the angle of twist (radian).

In this study, the torsional stiffness of each specimen was evaluated at two key stages:

1) Post-Cracking Stiffness (Kt_{post})

Kt_{post} is calculated by taking the difference in torque between the ultimate load (Tu) and the first visible crack load (Tcr), divided by the difference in their corresponding twist angles ($\theta u - \theta cr$), as expressed in:

$$Kt_{post} = \frac{(T_u - T_{cr})}{(\theta_u - \theta_{cr})} \quad (2)$$

Post-cracking stiffness represents the effective stiffness after cracking and before failure.

2) Ultimate Stiffness (Kt_{ult})

Kt_{ult} is calculated by dividing the ultimate torque by its associated twist angle:

$$Kt_{ult} = \frac{T_u}{\theta_u} \quad (3)$$

This value reflects the residual stiffness at peak loading just before failure. Table VI summarizes the computed Kt_{post} and Kt_{ult} values, along with the retention ratios (Kt_{ult}/Kt_{post}). These parameters were used to assess the torsional degradation and the effectiveness of each strengthening technique.

TABLE VI. TORSIONAL STIFFNESS AND RETENTION RATIOS OF THE TESTED SPECIMEN

Specimen	Kt_{post} (kN.m/rad)	Kt_{ult} (kN.m/rad)	*Kt* retention ratio (%)
CRS0	1369	1766	129
CRSNS2	1051	2029	193
CRSNS4	896	2150	240
CRSNB2	1749	2123	121
CRSNB4	1811	2258	125

IV. DISCUSSION

A comparison with previous studies shows that several investigations have examined the performance of reinforced concrete beams strengthened using NSM techniques. In [22, 23], a continuous spiral NSM method with steel wire ropes significantly improved the torsional performance of RC beams, with ultimate torque increasing by up to 140% relative to the control beam, depending on the spiral spacing. Similarly, in [24], beams strengthened with external steel rings and NSM longitudinal bars exhibited enhanced ductility and cracking behavior, especially at reduced spacing intervals. Authors in [25] explored the use of CFRP and steel NSM bars with different configurations and concluded that the four-bar NSM arrangements yielded superior torsional resistance and ductility while reducing the crack widths. Furthermore, authors in [26] confirmed that replacing steel NSM bars with CFRP strips improved both the energy absorption and ductility under pure torsion, with a noticeable reduction in crack propagation and an increased ultimate torque.

Moreover, while previous experimental studies have extensively explored NSM steel or FRP techniques, the current investigation adds basalt bars to the NSM system. The findings revealed that basalt bars, despite having lower stiffness than the steel bars, contributed positively to the torsional strength and post-cracking behavior when used in NSM applications. Therefore, this study not only aligns with the enhancement trends reported in earlier works [23-26], but also fills a critical research gap by evaluating the torsional efficiency of basalt-based NSM systems under repeated pure torsion, a subject that has received limited attention in prior literature.

V. CONCLUSIONS

Based on the results and analysis, the main conclusions drawn from this study are:

- Relative to the unstrengthened control beam, the ultimate torque rose by 16.5% in the two-sided configuration (CRSNS2) and by 30.4% in the four-sided configuration (CRSNS4).
- The Near-Surface Method (NSM) basalt-reinforced beams showed enhanced performance, although to a lower degree. The ultimate torque increased by about 33.0% for the two-sided configuration (CRSNB2) and 46.1% for the four-

sided configuration (CRSNB4), indicating a significant improvement relative to the reference beam.

- The steel NSM bars exhibited better crack resistance and a delayed first crack because of their enhanced stiffness and yielding capability. Conversely, the basalt-reinforced beams showed a quicker cracking development and greater crack widths due to the reduced stiffness and brittle behavior of the basalt bars.

Overall, the NSM steel bars proved more effective in boosting the torsional capacity, while the basalt bars provided valuable improvements in the stiffness retention and post-cracking behavior.

REFERENCES

[1] *Building Code Requirements for Structural Concrete and Commentary*, ACI 318-19, American Concrete Institute, Farmington Hills, MI, 2019.

[2] ACI Committee 408, *State-of-the-Art Report: Bond under Cyclic Loads*, 6th ed., vol. 88. Farmington Hills, MI: American Concrete Institute, 1992.

[3] G. Al-Bayati, R. Al-Mahaidi, and R. Kalfat, "Experimental investigation into the use of NSM FRP to increase the torsional resistance of RC beams using epoxy resins and cement-based adhesives," *Construction and Building Materials*, vol. 124, pp. 1153–1164, Oct. 2016, https://doi.org/10.1016/j.conbuildmat.2016.08.095.

[4] G. Al-Bayati, R. Al-Mahaidi, and R. Kalfat, "Torsional strengthening of reinforced concrete beams using different configurations of NSM FRP with epoxy resins and cement-based adhesives," *Composite Structures*, vol. 168, pp. 569–581, May 2017, https://doi.org/10.1016/j.compstruct.2016.12.045.

[5] K. F. K. Hassanien, "Strengthening of reinforced concrete beams using near-surface mounted FRP," *International Journal of Engineering Science and Innovative Technology*, vol. 4, no. 5, pp. 231–237, Sep. 2015.

[6] K. N. Rahal and H. A. Rumaih, "Tests on reinforced concrete beams strengthened in shear using near surface mounted CFRP and steel bars," *Engineering Structures*, vol. 33, no. 1, pp. 53–62, Jan. 2011, https://doi.org/10.1016/j.engstruct.2010.09.017.

[7] A. A. Abdul Samad, D. R. Hassen, N. Mohamad, A. N. Attiyah, J. Jayaprakash, and P. Mendis, "Shear Rehabilitation of RC Deep Beams using NSM CFRP Anchor Bars," *MATEC Web of Conferences*, vol. 103, 2017, Art. no. 02010, https://doi.org/10.1051/matecconf/201710302010.

[8] M. A. Anis A. and M. Thaer Matlab, "Shear Strengthening of RC without Stirrups for Deep Beams with Near Surface Mounted CFRP Rods," *International Journal of Engineering Research & Technology*, vol. 04, no. 06, pp. 545–547, Jun. 2015.

[9] F. Elgabbas, E. A. Ahmed, and B. Benmokrane, "Physical and mechanical characteristics of new basalt-FRP bars for reinforcing concrete structures," *Construction and Building Materials*, vol. 95, pp. 623–635, Oct. 2015, https://doi.org/10.1016/j.conbuildmat.2015.07.036.

[10] A. Serbescu, M. Guadagnini, and K. Pilakoutas, "Mechanical Characterization of Basalt FRP Rebars and Long-Term Strength Predictive Model," *Journal of Composites for Construction*, vol. 19, no. 2, Apr. 2015, Art. no. 04014037, https://doi.org/10.1061/(asce)cc.1943-5614.0000497.

[11] C. C. Gowda, J. A. O. Barros, and M. Guadagnini, "Experimental study of torsional strengthening on thin walled tubular reinforced concrete structures using NSM-CFRP laminates," *Composite Structures*, vol. 208, pp. 585–599, Jan. 2019, https://doi.org/10.1016/j.compstruct.2018.10.050.

[12] N. Habeeb Askandar and A. Darweesh Mahmood, "Torsional Strengthening of RC Beams with Near-Surface Mounted Steel Bars," *Advances in Materials Science and Engineering*, vol. 2020, no. 1, Jan. 2020, Art. no. 1492980, https://doi.org/10.1155/2020/1492980.

[13] M. Alrawi and M. Mahmood, "Strengthening Reinforced Beams Subjected to Pure Torsion by Near Surface Mounted Rebars," *Anbar Journal for Engineering Sciences*, vol. 13, no. 1, pp. 13–22, Oct. 2022, https://doi.org/10.37649/aengs.2022.175876.

[14] M. I. Ali and A. A. Al-Azzawi, "Finite element analysis of RC beams strengthened with near-surface mounted reinforcement bars under pure torsion," *IOP Conference Series: Earth and Environmental Science*, vol. 1232, no. 1, Sep. 2023, Art. no. 012026, https://doi.org/10.1088/1755-1315/1232/1/012026.

[15] *Portland Cement*, Specifications No. 5, Iraqi specifications, Baghdad, Iraq, 1984.

[16] *Specification for Portland Cement*, ASTM C150/C150M-22, ASTM International, West Conshohocken, PA, 2022.

[17] *Aggregate from Natural Sources for Concrete and Construction*, Specifications No. 45, Iraqi Specifications, Baghdad, Iraq, 1984.

[18] *Testing concrete*, BS 1881-116:1983 British Standards Institution, London, Jan. 1983.

[19] *Standard Test Method for Flexural Strength of Concrete (Using Simple Beam With Center-Point Loading)*, ASTM C293/C293M-16 ASTM International, West Conshohocken, PA, 2016.

[20] *Test Method for Splitting Tensile Strength of Cylindrical Concrete Specimens*, ASTM C496/C496M-17 ASTM International, West Conshohocken, PA, 2017.

[21] S. B. Kadhum and A. H. Al-Zuhairi, "The Effect of Construction Joints on the Behavior of Reinforced Concrete Deep Beams," *Engineering, Technology & Applied Science Research*, vol. 14, no. 4, pp. 16083–16089, Aug. 2024, https://doi.org/10.48084/etasr.7896.

[22] A. A. Elghany, M. Elsayed, A. Elsayed, and A. Shaheen, "Enhancement of the Shear Capacity of RC Deep Beams with Ultra-High Performance Fiber-reinforced Concrete," *Engineering, Technology & Applied Science Research*, vol. 15, no. 1, pp. 20418–20424, Feb. 2025, https://doi.org/10.48084/etasr.9792.

[23] N. H. Askandar and A. D. Mahmood, "Torsional Strengthening of RC Beams with Continuous Spiral Near-Surface Mounted Steel Wire Rope," *International Journal of Concrete Structures and Materials*, vol. 14, no. 1, Dec. 2020, Art. no. 7, https://doi.org/10.1186/s40069-019-0386-4.

[24] M. I. Ali and A. A. Al-Azzawi, "Finite element analysis of RC beams strengthened with near-surface mounted reinforcement bars under pure torsion," *IOP Conference Series: Earth and Environmental Science*, vol. 1232, no. 1, Sep. 2023, Art. no. 012026, https://doi.org/10.1088/1755-1315/1232/1/012026.

[25] S. F. M. Razak, M. A. Ahmad, A. A. A. Samad, and M. A. Alqurashi, "Strengthening of RC beams subjected to pure torsion using near surface mounted (NSM) CFRP bars," *Journal of Engineering Science and Technology*, vol. 17, no. 3, pp. 2059–2076, Jun. 2022.

[26] A. M. Rteil and F. F. Haddad, "Torsional behavior of high-strength concrete beams," *Engineering Structures*, vol. 19, no. 11, pp. 936–945, Nov. 1997.